Materials Advances

ROYAL SOCIETY OF CHEMISTRY

PAPER

View Article Online
View Journal

Cite this: DOI: 10.1039/d6ma00579a

Carbon dots derived from polyurethane waste for photocatalytic dye removal

Tomaz Alves dos Santos Lima,[a] Isabelly Antônia de Souza Rodrigues,[a] Paulo Salles Neto,[a] Letícia Develly,[b] Willian X. C. Oliveira[b] and Raquel Vieira Mambrini*[a]

Received 24th April 2026,
Accepted 15th June 2026

DOI: 10.1039/d6ma00579a

rsc.li/materials-advances

Carbon dots (CDs) were synthesized from polyurethane (PU) waste through a simple and sustainable hydrothermal route. The synthesis promotes carbonization and nitrogen incorporation from the polymer backbone, resulting in stable, quasi-spherical nanoparticles with graphitic domains and green photoluminescence. The CDs exhibited excellent colloidal stability, strong absorption at 284 nm ($\pi \rightarrow \pi^*$), and stable emission over 6 months. Their photocatalytic activity was evaluated in the degradation of methylene blue (MB) and other dyes under UV-C irradiation in the presence of H_2O_2. The optimized material (200CD14) achieved 98.3% MB removal and 92% reduction in total organic carbon, confirming efficient mineralization. Radical scavenging assays indicated the participation of both $O_2^{\bullet -}$ and $^{\bullet}OH$ species in the process. The CDs maintained over 80% activity after five reuse cycles, demonstrating their robustness and potential for wastewater treatment. This work demonstrates the successful conversion of PU waste into functional nanomaterials, offering a practical approach within green chemistry and the circular economy for valorizing polymeric residues.

Introduction

The development of new materials drives advances across many scientific fields, particularly for technological and sustainable applications. In this context, nanomaterials exhibit unique physicochemical properties, attributed to their high surface-to-volume ratio and quantum confinement effects, which are promising for photocatalysis and advanced oxidation processes. Among carbon-based nanomaterials, carbon dots (CDs) have attracted considerable interest due to their structural versatility, chemical stability, and biocompatibility.[1] CDs belong to the class of quantum dots and are typically spherical nanoparticles with diameters below 10 nm; they exhibit strong fluorescence, high water solubility, and the possibility of surface functionalization with reactive groups.[2] These features make CDs promising for applications in bioimaging,[3] fluorescent sensors,[4] light-emitting devices,[5] and photocatalysis.[6]

The classification of carbon-based nanomaterials remains an open and actively debated topic in the literature. The term "carbon dots" encompasses a broad structural family, including graphene quantum dots, carbon quantum dots, carbon nanodots, and carbonized polymer dots, each distinguished by their carbon core structure, degree of graphitization, and surface chemistry.[7–9] More recently, size-based criteria have been applied more strictly, with some authors preferring the designation "carbon nanostructures" for materials in which agglomeration yields particles exceeding 10 nm in all dimensions.[10]

A variety of synthetic routes have been explored for CD production and are commonly grouped into top-down[11] and bottom-up[3] approaches. Hydrothermal synthesis, a bottom-up strategy which by definition utilize controlled molecular assembly from atomic precursor, while top-down methods reduce macroscopic precursors to nanoscale dimensions *via* physical or chemical fragmentation and reassembly, both are critical for precisely tailoring the morphological and physicochemical properties of nanomaterials stands out for its operational simplicity, energy efficiency, and compatibility with organic precursors, including waste streams.

The literature highlights a wide variety of sustainable and unconventional precursors. Biogenic and biomass-derived materials have been extensively explored through hydrothermal and microwave-assisted synthesis, including amino acid mixtures,[3] chicken feathers,[12] lemon juice,[13] loblolly pine,[14] and folic acid.[15] Furthermore, industrial derivatives and byproducts, such as carbon black,[16] and general biomass carbon.[17] Beyond these natural precursors, synthetic polymers such as polyurethane (PU) are also explored.[17–19]

[a] Federal Center for Technological Education of Minas Gerais (CEFET-MG), Av. Amazonas 5253, Nova Suiça, Belo Horizonte, MG 30421-169, Brazil. E-mail: raquelmambrini@cefetmg.br
[b] Department of Chemistry, Institute of Exact Sciences, Federal University of Minas Gerais (UFMG), Av. Antônio Carlos 6627, Pampulha, Belo Horizonte, MG 31270-901, Brazil

The continuous accumulation of non-biodegradable polyurethane (PU) waste has emerged as a critical environmental issue, reinforcing the need for efficient valorization strategies aligned with circular economy principles.[20] PU is a particularly advantageous precursor as its polymer structure is not only carbon-rich but also inherently contains nitrogen and oxygen within its urethane linkages. This built-in N and O doping generates a functionalized surface that prevents nanoparticle agglomeration through electrostatic stabilization and enhances interactions with diverse chemical environments. Also, these surface heteroatoms play a crucial role in passivating surface defects, thereby modulating the electronic structure and boosting the overall photoluminescence performance of this material.[21] This chemical composition enables the one-pot, *in situ* synthesis of CDs, which are widely reported to exhibit enhanced optical properties and surface reactivity, thereby increasing their potential for photocatalytic applications.[22]

Building upon these electronic properties, the redox capabilities of carbon dots are strictly governed by their specific surface chemistry. Heteroatoms and functional groups on the CD surface, such as those derived from urethane linkages, serve as essential active catalytic sites and charge traps. These localized surface states not only facilitate the separation of photogenerated electron–hole pairs but also promote rapid interfacial electron transfer to adsorbed aqueous species. Consequently, this precise surface chemistry significantly enhances ROS generation, establishing a direct link between the structural functionalization of the carbonaceous matrix and its macroscopic catalytic efficiency.[23]

Concurrently, the presence of industrial dyes in aqueous effluents represents a growing environmental challenge due to their toxicity, chemical stability, and resistance to biological degradation. Methylene blue (MB), for example, is a cationic dye widely employed and frequently detected in wastewater; it is characterized by high solubility, persistence, and environmental impact even at low concentrations.[24] Photocatalysis, particularly when mediated by semiconductor materials such as CDs, has proven to be an effective approach for dye degradation in aqueous media.

The application of carbon dots (CDs) as metal-free photocatalysts for environmental remediation is a well-established research area.[25] Their catalytic activity is attributed to their semiconductor-like ability to generate electron–hole pairs (e^-/h^+) upon light absorption. These charge carriers react with adsorbed O_2 and H_2O to produce Reactive Oxygen Species (ROS),[10,26] associated with the radical hydroxyl ($^\bullet OH$) and superoxide ($O_2^{\bullet -}$). These are potent oxidizing agents that can effectively mineralize recalcitrant organic pollutants, such as methylene blue, into simpler products.[6] Furthermore, the high surface area and tunable electronic properties of CDs, often enhanced by doping, promote efficient charge separation and broaden light absorption, thereby improving overall photocatalytic performance.[6]

Although polyurethane-derived carbon dots have been previously reported,[27,28] their application often relies on composite systems,[29] semiconductor supports,[28] or metal-containing materials.[30] In this work, polyurethane waste is directly converted into metal-free and support-free carbon dots that act as the sole photocatalyst for dye degradation, providing a simple and sustainable route for waste valorization and wastewater treatment.

Results and discussion

Preparation and characterization of the CDs

Carbon dots (CDs) were synthesized from polyurethane waste *via* a hydrothermal route at various temperatures and reaction times to investigate the impact of these parameters on the physicochemical and optical properties of the resulting nanomaterials. Five experimental trials were performed, and pH, conductivity, and fluorescence were analyzed (Table 1).

Entries 1 and 2, carried out at 160 °C (160CD14) and 180 °C (180CD14) for 14 hours, produced materials with final pH values between 5.9 and 6.1 and low electrical conductivity (15 to 126 μS), lacking visible photoluminescence. While initial measurements suggested that electrical conductivity was a preliminary indicator of overall surface ionization, samples synthesized at 200 °C showed a more complex dependence on reaction time. Entry 4 (200CD14, 14 h) displayed a conductivity of 282 μS and distinct photoluminescence. Conversely, Entry 3 (200CD7, 7 h) exhibited lower conductivity (64 μS), and Entry 5 (200CD18, 18 h) presented the highest conductivity (372 μS) but a complete loss of photoluminescence. This behavior indicates that although elevated temperatures favor initial CD formation,[27,31] excessive reaction times induce over-carbonization. Such extensive thermal treatment likely degrades the specific fluorophoric surface states and functional groups responsible for emission, converting them into non-luminescent structures or promoting the aggregation of surface defects. This maintains a high concentration of charged species that contribute to conductivity but completely quenches fluorescence. This mechanism is consistent with recent literature emphasizing that CD photoluminescence is strictly governed by the precise nature and preservation of specific surface functionalities rather than the absolute extent of functionalization.[32] Therefore, reaction time must be carefully optimized to balance carbonization with the retention of emissive surface states.

After excitation at 254 nm for 10 minutes, the UV-vis spectrum of the selected CD dispersion (Fig. 1b) shows a strong

Table 1 Experimental conditions used in the preparation of the CDs: sample name, temperature (°C), reaction time (h), final pH, electrical conductivity (μS), and observed photoluminescence

Entry	Name	T (°C)	t (h)	pH	Conductivity (μS)	Fluorescence observed
1	160CD14	160	14	6.1	15	No[a]
2	180CD14	180	14	5.9	126	No[a]
3	200CD7	200	7	5.9	64	Yes
4	200CD14	200	14	6.0	282	Yes
5	200CD18	200	18	4.8	372	No[a]

[a] Entries 1, 2, and 5 showed no detectable photoluminescence under UV-C irradiation and are more appropriately classified as carbonized nanoparticles. The term "CD" was retained for consistency within the synthesis series.

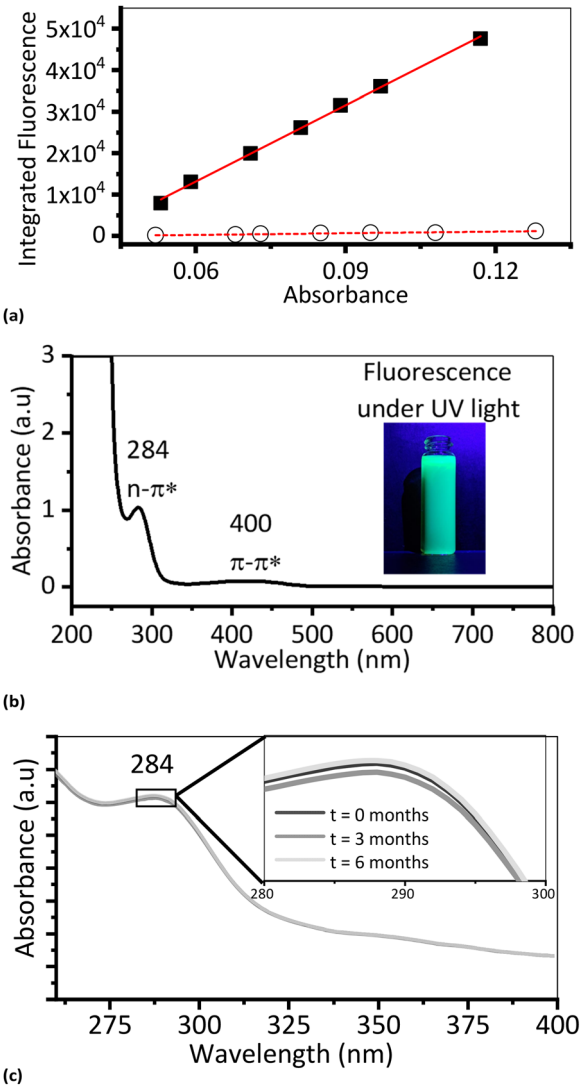

Fig. 1 (a) Plots of absorbance at 350 nm and integrated fluorescence for carbon dots (circles) solution and for quinine sulfate in 0.1 mol L^{-1} H_2SO_4 (squares) with linear adjustment (solid red line for sulfate quinine and dotted red line for carbon dot solution), (b) UV–vis spectrum of CD (200CD14) after 10 minutes of irradiation at 365 nm. (c) spectrum after 3 and 6 months of storage. The insert in (b) shows fluorescence under 365 nm UV-C light after dark storage.

absorption band at 284 nm, assigned to π → π* transitions of aromatic sp^2 domains[18] and a secondary band around 400 nm attributed to n → π* transitions of surface groups.[33] The intense green photoluminescent emission under UV excitation is characteristic of CDs bearing surface functional groups[33] and is also often attributed to the quantum confinement effect,[34] where smaller nanoparticles typically exhibit emission in the blue-to-green region.[7] These features confirm the conversion of the polymeric residue into functional nanomaterials.

During a six-month period, photo stability was measured after storage under normal laboratory lighting conditions. The CD dispersion retained its photoluminescence at 3 and 6 months (Fig. 1c), indicating good optical stability for potential practical applications.[35]

Fourier-transform infrared spectroscopy (FTIR, Fig. 3a) revealed structural transformations from the polyurethane precursor to the carbon dots. Comparison of spectra indicated a change in intensity of the carbonyl (C═O) stretching band at 1711 cm^{-1},[36] (present in the polyurethane), reflecting the conversion of these linkages during hydrothermal treatment.[36] The band assigned to NH bending at 1534 cm^{-1} is observed in PU and in the CD, suggesting partial preservation of nitrogen-containing functionalities.[36] The NH stretching band, initially at 3393 cm^{-1} in the precursor, shifts to 3363 cm^{-1} in the CD and decreases in intensity, indicating changes in the chemical environment of amino groups.[27] The CH_2 stretching at 2867 cm^{-1} remains unchanged, while the band at 1086 cm^{-1} (associated with C–O or C–N stretching) shows changes in pattern and relative intensity, evidence of structural reorganization and the formation of new surface functional groups.[14,37] Overall, these FTIR changes confirm that the original polyurethane structure (characterized by carbonyl and NH linkages) was extensively modified, producing a functionalized carbonaceous material.

The fluorescence quantum yield (QY) of the Carbon Dots was determined following the comparative procedure using quinine sulfate in 0.1 mol L^{-1} H_2SO_4 as the reference standard, according to the classical methodology reported by Würth *et al.* (2013).[38] The photoluminescence (PL) and photoluminescence excitation (PLE) spectra (Fig. 2) showed emission and excitation maxima at 418 nm and 350 nm, respectively, enabling direct calculation of the QY from the slope ratio of integrated fluorescence *versus* absorbance (Fig. 1a). The Carbon Dots exhibited a very low quantum yield of 1.27%, which is characteristic of materials synthesized without surface passivation, where non-radiative decay pathways dominate. Although the sample displays a clear green fluorescence under UV light (Fig. 1b), the low QY indicates that most of the absorbed photon energy is not returned as radiative emission. Instead, the excited-state population undergoes extensive non-radiative relaxation, including photoinduced quenching, vibrational relaxation, electron–phonon coupling, and even partial energy dissipation as non-radiative thermal loss.[31] While some of this energy is indeed lost to simple dissipation, a significant fraction can be redirected into charge-separation processes and surface redox pathways, supporting the generation of reactive oxygen species under irradiation.[6,39]

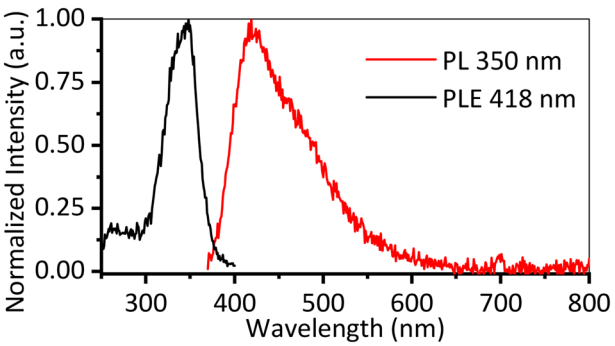

Fig. 2 PL (350 nm, in red) and PLE (418 nm, in black) spectra for the CD solution (200CD14).

Thermogravimetric analysis (TG, Fig. 3b) shows that the polyurethane precursor decomposes in two main stages: the first (200–400 °C) corresponds to about 50% mass loss related to degradation of urethane groups and side-chain fragments; the second stage (>400 °C) an additional mass loss of approximately 40% attributed to ester groups from the polyol, thus resulting in the complete degradation of the polymer.[40] Conversely, the carbon dots present a distinct TG profile: up to 300 °C, there is mass loss likely due to residual water and residual uretanic fragments. A second mass loss between 300–450 °C indicates the formation of a more thermally stable carbonaceous material with a denser nanometric structure and graphitic cores, typical of hydrothermally obtained carbon material.[40,41]

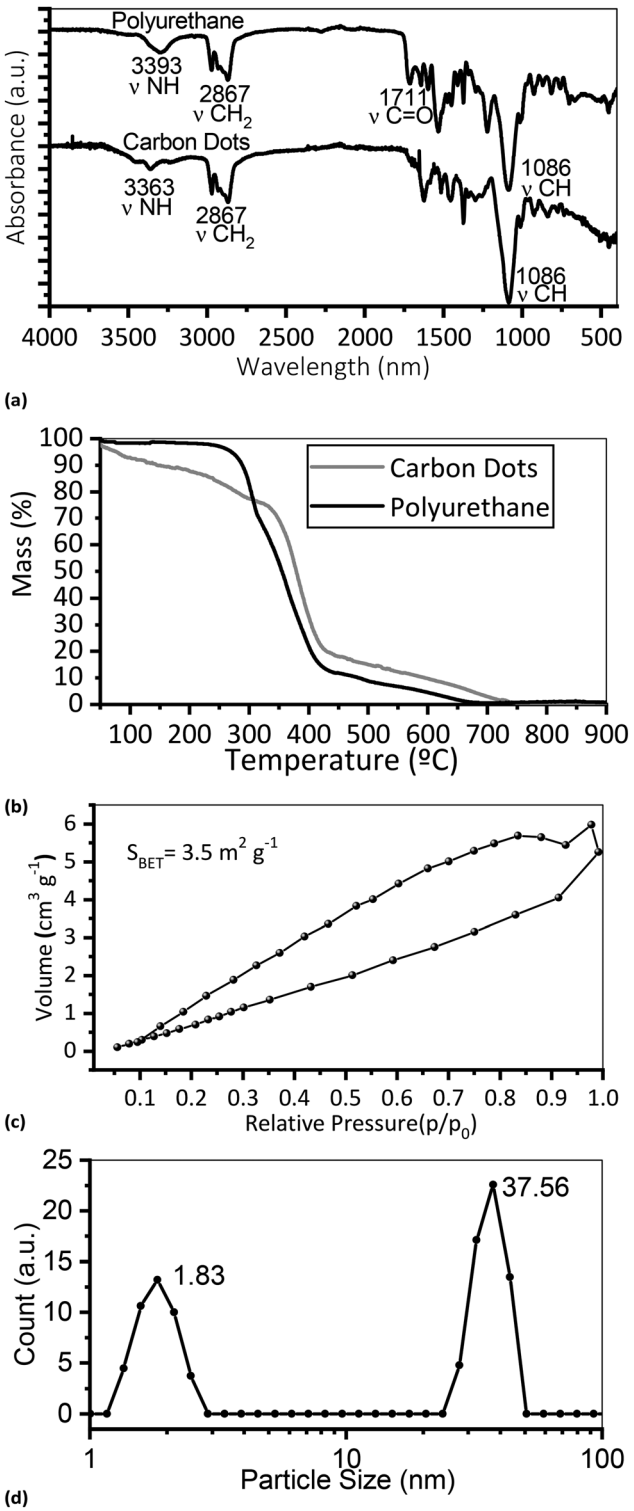

Fig. 3 (a) FTIR spectra of polyurethane and CD; (b) thermogravimetric (TG) curves of polyurethane and CD; (c) nitrogen adsorption–desorption isotherm of CD; (d) particle size distribution of CD. CD corresponds to material 200CD14.

The nitrogen adsorption–desorption isotherm (Fig. 3c) for the CD is classified as type III with a slight hysteresis, suggesting low overall N_2 affinity but the presence of accessible porous regions.[16,42] The calculated specific surface area was 3.5 $m^2 g^{-1}$, a value consistent with CDs produced by hydrothermal routes without subsequent physical or chemical activation. Particle size analysis (Fig. 3d) revealed two distinct distributions: a minor population centered at 1.8 nm, attributable to individual carbon dots, and a larger population peaked around 37 nm, indicative of agglomerates formed from the smaller nanoparticles confirming a nanometric dispersed material with a tendency to cluster.[37]

Scanning electron microscopy (SEM) images (Fig. 4) show heterogeneous structures with regions of agglomeration. These aggregates form porous, cluster-like structures that can enhance photocatalytic processes by increasing the surface area and generating adsorption/charge-transfer sites.[25,37] Energy-dispersive X-ray spectroscopy (EDS) associated with the SEM images indicates a high carbon concentration in the sample, consistent with the carbonaceous nature of the nanomaterials derived from the polymeric precursor.[15,43]

The primary nanoparticles identified by dynamic light scattering, with an average size of approximately 1.8 nm, are consistent with the classical definition of carbon dots.[2] In contrast, the larger structures observed by TEM, around 500 nm, are attributed to agglomerates formed by particle clustering during drying, as commonly reported for hydrothermally synthesized CDs.[37] Therefore, the term "carbon dots" is retained throughout this work to refer to the primary nanoparticulate species, while acknowledging the classification complexity of this class of carbon-based nanomaterials.[7–9]

The TEM image (Fig. 5c) shows lattice fringes with an interplanar spacing of approximately 0.19 nm. Similar lattice spacings have been reported for carbon dots in the literature, indicating the presence of partially ordered carbonaceous/graphitic-like domains.[44–46]

The crystalline structure of CD directly influences its electronic states and, consequently, its photoluminescent behavior. Graphitic domains function as localized quantum confinement regions, modulating the electronic density of states and the wavelengths of emission. Variations in local electronic structure and surface chemistry, therefore, enable tuning of CD photoluminescence.[21,47,48]

Zeta potential measurements (Fig. 6) indicate that the CD surface charge depends strongly on pH. The CD exhibits a

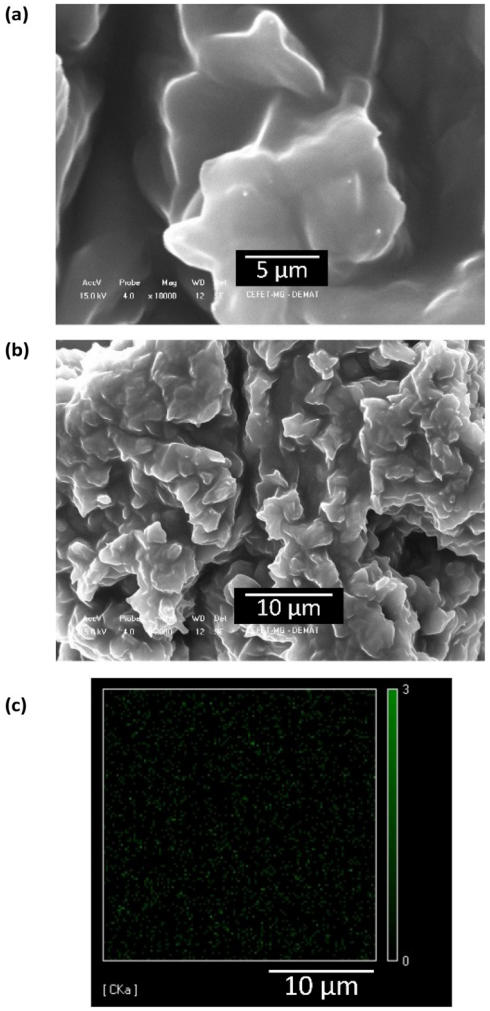

Fig. 4 SEM images of sample 200CD14 at different magnifications: (a) ×10.000, (b) ×5.000, and (c) EDS elemental mapping showing carbon (green signal).

zero-zeta potential around pH ≈ 7 (point of zero charge), positive values up to +11 mV at pH 2, and negative values down to about −6 mV at pH 12.[49] This pH-dependent surface charge behavior is essential for anticipating eslectrostatic interactions with charged pollutants.[18]

Application of the CD in pollutant removal

Following physicochemical characterization, the CD's photocatalytic performance was evaluated for the oxidative degradation of industrial dyes using various dyes as the model compound.[50,51] Photocatalytic assays were conducted under UV-C irradiation in the presence of hydrogen peroxide. Fig. 7.a summarizes dye removal in the system containing CD + H_2O_2 + UV-C + dye. In the presence of anionic dyes, the CD achieved removals of 36.4% (methyl yellow), 49.1% (methyl red), 62.5% (methyl orange), and 98% (bromophenol blue). For cationic dyes, fuchsin and methylene blue were removed with efficiencies of 89.9% and 98.3%, respectively, demonstrating generally good catalytic activity across structurally diverse dyes.[52,53] One possible contributor to dye removal is adsorption mediated by electrostatic interactions.

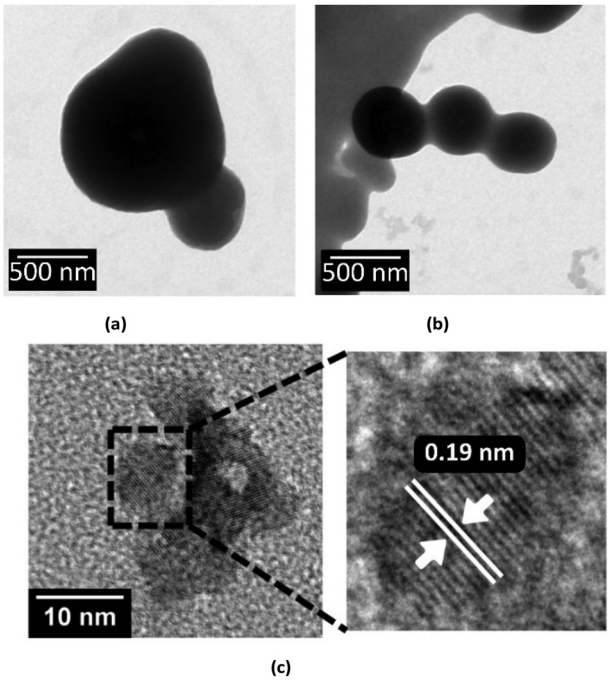

Fig. 5 TEM images of carbon dots (200CD14): (a, b) TEM micrographs showing particle morphology and aggregation, and (c) high-resolution TEM (HRTEM) image revealing lattice fringes with a d-spacing of 0.19 nm, indicating the presence of graphitic domains.

According to the zeta potential measurements (Fig. 6), the CDs exhibit a slightly positive surface charge at the reaction pH (∼6), with a zeta potential of approximately +4 mV. This condition may favor the initial adsorption of anionic dyes through weak electrostatic attraction while slightly disfavoring the adsorption of cationic dyes. However, the photocatalytic results do not show a direct correlation with the dye charge, as high removal efficiencies were observed for both anionic and cationic dyes. For example, bromophenol blue (anionic) and methylene blue (cationic) exhibited removal efficiencies above 98%. These findings indicate that electrostatic interactions alone cannot explain the observed behavior. The degradation performance is likely governed by a combination of intermolecular interactions between the dye molecules and the functional groups present on the CD surface, as well as oxidation pathways promoted by photocatalytically generated reactive oxygen species.[32,53–55]

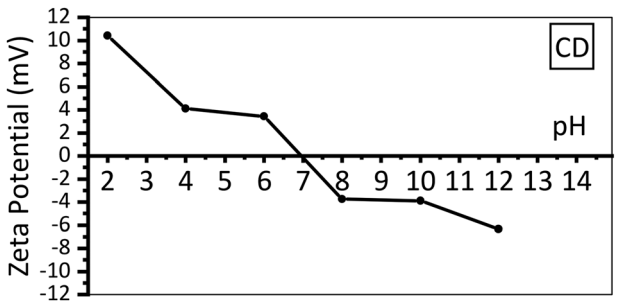

Fig. 6 Zeta potential of CD (200CD14) as a function of pH.

Kinetic tests (Fig. 7b) for the three dyes with the highest removal rates (fuchsin, bromophenol blue, and methylene blue) show that removals exceeded 90% within 180 minutes of irradiation, indicating performance comparable to reported systems.[50] Initially, control tests were performed (Fig. 8a). The control experiments showed methylene blue removals of 42.0% with UV-C irradiation alone, 45.7% with UV-C/H_2O_2, 62.1% with CDs alone, and 73.2% with the combined UV-C/CDs system. The highest removal efficiency (98.3%) was achieved using the complete UV-C/CDs/H_2O_2 system. These results demonstrate that neither photolysis nor oxidation by H_2O_2 alone can account for the observed degradation efficiency. Instead, a significant synergistic effect is observed when CDs, UV-C irradiation, and H_2O_2 are combined, indicating that the CDs actively participate in the generation of reactive species responsible for the enhanced degradation of methylene blue.

The degradation kinetics of methylene blue (Fig. 8b) were over 180 minutes, accompanied by quantification of total organic carbon (TOC). Color removal reached 98.3% after 180 minutes, with a simultaneous TOC reduction of 92%, evidence that the process promoted significant mineralization of the pollutant rather than mere decolorization.[56,57]

While the photocatalytic removal of dyes using semiconductor quantum dots (such as ZnS or CdSe) is well-documented,[58,59] these materials often rely on toxic heavy metals or require complex synthesis methods involving hazardous precursors. Regarding Carbon Dots (CDs), although they are recognized as eco-friendly alternatives, most of the literature employs them as photosensitizers or co-catalysts in composite systems typically supported on TiO_2 or ZnO rather than as primary active species. In distinct contrast, this work demonstrates the efficacy of waste-derived CDs as standalone, metal-free photocatalysts. By valorizing polyurethane residues as a carbon source, we present a sustainable, ''support-free'' approach that simplifies the catalytic system while maintaining high degradation efficiency, thus addressing both waste management and water remediation challenges simultaneously.

To elucidate the degradation mechanism, radical scavenging experiments were performed (Fig. 8b). Addition of DMSO (a selective •OH scavenger[26] led to only a 5% drop in removal efficiency, while methanol (also a •OH scavenger)[24] produced a about 25% decrease. Ethanol, which can scavenge both •OH and superoxide radicals ($O_2^{\bullet -}$),[54] produced the largest inhibition

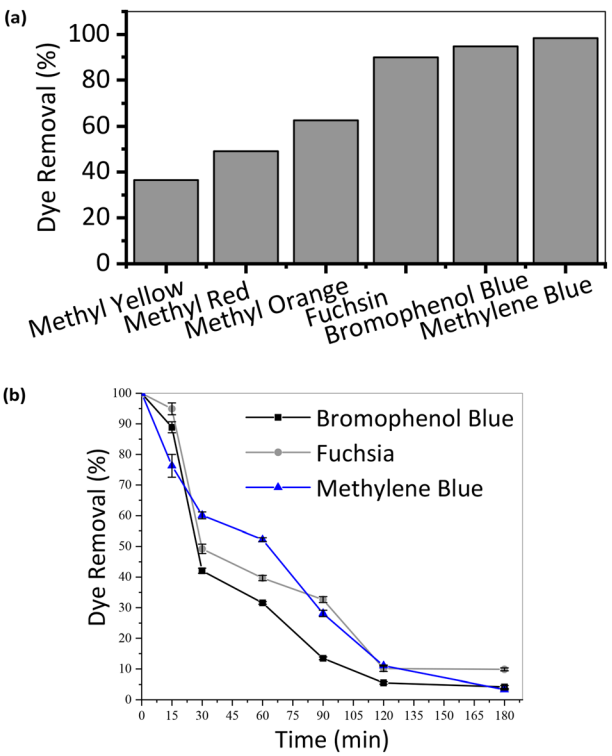

Fig. 7 (a) Dye removal efficiency of CD (200CD14) for different dyes; (b) removal kinetics for the three dyes with the highest efficiency under UV-C irradiation.

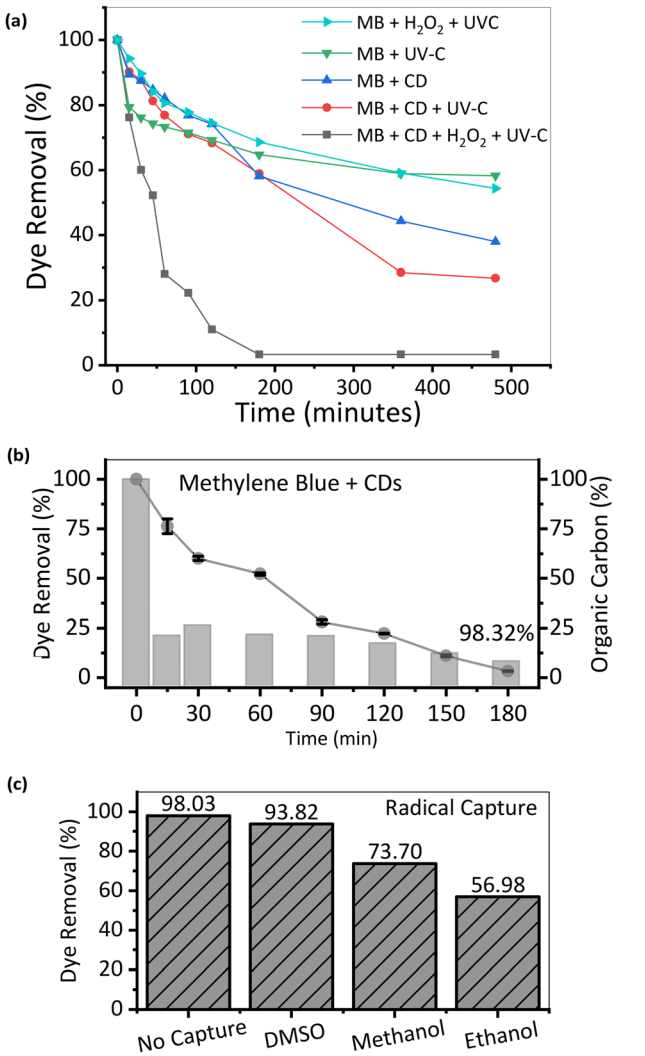

Fig. 8 (a) Comparison of MB removal efficiencies obtained using UV-C irradiation, H_2O_2/UV-C, CDs, CDs/UV-C, and CDs/H_2O_2/UV-C systems. (b) Kinetics of methylene blue degradation over 180 minutes and variation in total organic carbon (TOC). (c) Radical scavenging tests using DMSO, methanol, and ethanol.

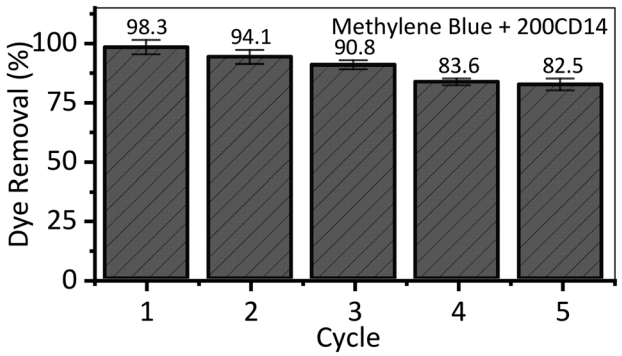

Fig. 9 Stability and reusability of CD (200CD14) for methylene blue removal over five consecutive cycles.

(~42%). This pattern indicates that reactive oxygen species play a central role in the degradation process, with superoxide radicals ($O_2^{\bullet -}$) appearing to be the dominant oxidizing species and hydroxyl radicals ($^{\bullet}OH$) providing a secondary contribution. The scavenger experiments therefore support a ROS-mediated degradation pathway under the investigated conditions.[60]

Reusability tests were performed for five consecutive photocatalytic cycles (Fig. 9) without intermediate purification, drying or reactivation only fresh dye aliquots were added under the same operating conditions. The material exhibited a small loss of activity across cycles, with a maximum decrease of ~15% after five uses, associated to catalyst leaching because of laboratory conditions, demonstrating high structural and functional robustness that is favorable for potential large-scale application.[26,61]

ESI-MS analysis over the reaction time (Fig. 10) revealed that the signal at *m/z* 285, associated with methylene blue, decreased progressively and disappeared after 60 minutes consistent with full degradation of the parent dye.[52] From 15 minutes onwards, fragment ions at *m/z* 234, 261, 141 and others were detected and attributed to oxidation intermediates;[62] these fragments presented low intensity, suggesting only trace concentrations of such intermediates.[62,63] These observations agree with TOC data and further corroborate the efficient oxidative degradation and mineralization pathway promoted by the CDs under UV-C irradiation.

Taken together, the results indicate that dye removal by the CDs occurs *via* a combined mechanism of adsorption and photocatalysis. Surface functional groups such as –OH, –COOH

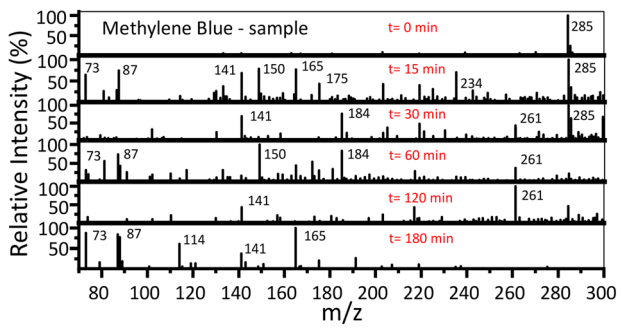

Fig. 10 ESI(+)-MS spectra for the degradation of methylene blue (50 mg L^{-1}) in the presence of CD (200CD14) and H_2O_2.

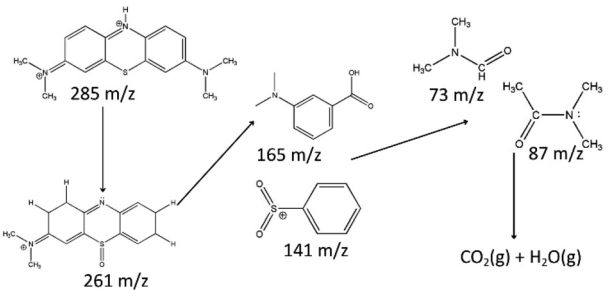

Fig. 11 Proposed degradation pathway of Methylene Blue, highlighting the major intermediates identified by mass spectrometry at *m/z* 285, 261, 165, 141, 87, and 73 leading to mineralization.

and $-NH_2$ promote adsorption especially for anionic dyes *via* electrostatic interaction[42] and, under UV-C in the presence of H_2O_2, the CDs act as semiconductor photocatalysts: upon photoexcitation electron–hole pairs are generated and react with water and peroxide to form reactive oxygen species (ROS) such as hydroxyl radicals ($^{\bullet}OH$) and superoxide ($O_2^{\bullet -}$).[6,54] These ROS oxidize dye molecules, breaking aromatic structures and driving partial to substantial mineralization. The detection of oxidation intermediates and the observed reduction of TOC during photocatalytic assays confirm the effective operation of this combined mechanism.[50,57]

The proposed degradation pathway, Fig. 11, evidences that the process is driven by the successive fragmentation of the precursor molecule. The analysis of the formed intermediates predominantly highlighted the mass-to-charge ratio (*m/z*) peaks 285, 261, 165, 141, 87, and 73. The decay of the parent molecule (*m/z* 285)[63] initiates with oxidative attacks generating the intermediate at *m/z* 261, followed by the opening of aromatic rings and the formation of lower molecular weight byproducts (*m/z* 165 and 141).[62] Finally, the detection of aliphatic fragments at *m/z* 87 and 73 indicates an advanced oxidation stage, progressing towards the complete mineralization of organic compounds.

The excellent photocatalytic performance observed in this work, with degradation efficiencies above 90% for both anionic and cationic dyes, corroborates the low quantum yield, which reflects a photophysical regime in which the absorbed energy is largely directed to non-radiative channels, thereby increasing photocatalytic activity.[64]

Experimental

Preparation of the carbonaceous precursor

Polyurethane (PU) waste obtained from discarded flexible foams provided by a local mattress manufacturer was ground in a knife mill (model SL-30, Solab®) and sieved through a 30-mesh screen to produce a more homogeneous particle size distribution. The resulting powder was used as the carbonaceous precursor for the synthesis of carbon dots (CDs).

Preparation of carbon dots

The CDs materials were prepared *via* a hydrothermal route. In a typical procedure, approximately 2.0 g of PU powder was

dispersed in distilled water and transferred into a Teflon-lined stainless-steel autoclave. Reactions were conducted under different conditions of temperature (120, 140, 160, 180, and 200 °C) and reaction time (7, 12, 14, 18, and 24 h) to evaluate their influence on the yield and properties of the material. After cooling and separating *via* centrifugation, the suspensions obtained were centrifuged and subsequently filtered through 0.22 μm syringe filters. The colloidal dispersions were stored under refrigeration at 7 °C.

Characterization of the CDs

The optical stability of the colloidal dispersions was investigated by irradiation under UV-C light (254 nm) for 10 minutes, followed by acquisition of the UV-vis spectrum (Kasvi K37-UVVIS, 190–1100 nm). The same experiment was repeated after 3 and 6 months to study photoluminescence stability. Electrical conductivity and pH were measured using a Kasvi bench-top meter. Fourier-transform infrared spectroscopy (FTIR-ATR) was performed on dried solid samples using an IRPrestige-21 spectrometer (Shimadzu) in the 4000–400 cm^{-1} region. Thermogravimetric and derivative thermogravimetric analyses (TG/DTG) were carried out in synthetic air flow (50 mL min^{-1}) up to 900 °C, at a heating rate of 10 °C min^{-1}, using a DTG60H analyzer (Shimadzu). Textural properties were determined by nitrogen adsorption–desorption isotherms at 77 K using an Autosorb analyzer (Quantachrome Corp.), after degassing at 150 °C for 12 h. SEM images were obtained using a Shimadzu SSX-550 microscope. After drying aliquots of the dispersion, redispersing in acetone, and drop-casting onto silicon substrates, the samples were sputter-coated with gold. TEM images were obtained using a FEI Tecnai G2-20 SuperTwin microscope operated at 200 kV. Zeta potential and particle size distribution were determined at 25 °C using a Malvern Zetasizer Nano; for this analysis, 500 μL of dispersion was diluted in 20 mL of distilled water, sonicated for 30 minutes, and the pH was adjusted sequentially to 2, 4, 6, 8, 10, and 12 to build the surface charge curve. The fluorescence quantum yield (QY) was calculated using quinine sulfate (QY = 0.59 in 0.1 mol L^{-1} H_2SO_4) as reference, following a comparative method. For both the reference and the sample, absorbance was adjusted to 0.05–0.15 at 350 nm, and the integrated emission areas were plotted as a function of absorbance to obtain the respective slopes ($grad_R$ and $grad_S$). The quantum yield was then obtained using eqn (1), correcting for the refractive index of each solvent (n_S and n_R). This procedure ensured linearity, low inner-filter effects, and reproducibility of the emission response.

$$Q_s = Q_R \times \left(\frac{grad_S}{grad_R}\right) \times \left(\frac{n_S}{n_R}\right)^2 \quad (1)$$

Application of CDs in dye removal

The photocatalytic activity of the CDs was evaluated in the degradation of methylene blue (MB) under UV-C irradiation (254 nm). For each assay, 10 mL of a 100 ppm MB solution was mixed with 500 μL of CD dispersion and 300 μL of hydrogen peroxide at the natural pH (approximately 6), under continuous stirring. The degradation process was monitored by UV-vis spectroscopy by following the decrease in MB absorbance at 667 nm over time until equilibrium was reached. Control experiments were performed without a catalyst, in the absence of H_2O_2, and without irradiation. Additional tests were conducted using other dyes of varying structures, including methyl yellow, methyl red, methyl orange, bromophenol blue, and basic fuchsin, to compare performance and simulate industrial effluent conditions. The removal kinetics of the three dyes with the highest efficiency under visible-light irradiation were evaluated under the same conditions as for methylene blue, as described above. The reusability of the material was verified over five consecutive cycles without intermediate purification or reactivation, simply by adding a fresh dye solution under the same conditions. Radical scavenging assays were also performed with dimethyl sulfoxide (DMSO), methanol, and ethanol to identify the main reactive oxygen species involved in the degradation.[26] The total organic carbon (TOC) was measured using a Shimadzu TOC-L analyzer. The subproducts formed after oxidation were investigated by electrospray ionization mass spectrometry (ESI-MS) with direct injection in a Shimadzu LCMS-8050 triple quadrupole spectrometer (positive full scan, *m/z* 70–300, scan rate 476 μ s^{-1}, nebulizing gas N_2 at 3 L min^{-1}, heating gas air at 10 L min^{-1}, interface temperature 350 °C, desolvation line 250 °C, desolvation temperature 602 °C, flow 0.3 mL min^{-1} with 0.1% formic acid in methanol, injection volume 1 μL).

Conclusions

This work reports the hydrothermal conversion of post-consumer polyurethane foam waste into carbon dots (CDs) with photocatalytic activity. Optimization of the synthesis conditions identified 200 °C and 14 h as the most suitable parameters, yielding CDs with quasi-spherical morphology, graphitic domains, green photoluminescence, good colloidal stability, and pH-dependent surface charge. The optical properties remained stable over six months of storage.

Photocatalytic experiments under UV-C irradiation demonstrated efficient degradation of both anionic and cationic dyes, with removal efficiencies reaching 98.3% for methylene blue and TOC reduction of 92%, indicating substantial mineralization. Radical scavenging experiments revealed the participation of reactive oxygen species in the degradation process, with superoxide radicals playing a major role. The CDs also showed good reusability, retaining over 80% of their initial activity after five consecutive cycles without regeneration.

These findings demonstrate that polyurethane waste can be valorized as a low-cost carbon source for the production of functional nanomaterials. The resulting metal-free and support-free CDs represent a promising and sustainable platform for photocatalytic wastewater treatment.

Author contributions

Tomaz Alves dos Santos Lima: conceptualization, methodology, investigation, formal analysis, writing original draft. Raquel Vieira Mambrini: supervision, conceptualization, writing review and editing, funding acquisition, resources. Isabelly Antônia de Souza Rodrigues: investigation. Paulo Salles Neto: formal analysis. Letícia Develly: formal analysis. Willian X. C. Oliveira: formal analysis.

Conflicts of interest

There are no conflicts to declare.

Data availability

The datasets supporting the conclusions of this study, including detailed synthesis conditions, physicochemical characterization (UV-vis, Raman, FTIR, XRD, TEM/SEM), photocatalytic performance data, kinetic modeling, and TOC analyses, are provided within the article and its supplementary information (SI). Supplementary information is available. See DOI: https://doi.org/10.1039/d6ma00579a.

Further data and raw datasets are available from the corresponding author upon reasonable request.

Acknowledgements

CNPq, FAPEMIG, and CAPES supported this work. The authors thank CNPq (grant numbers 407188/2025-8 and 402302/2023-0) and FAPEMIG (grant numbers APQ-03705-23). Tomaz Lima thanks CEFET-MG for the scholarships granted. The authors acknowledge the Federal Center for Technological Education of Minas Gerais (CEFET-MG) for the institutional support and infrastructure.

Notes and references

1 N. Slepičková Kasálková, P. Slepička and V. Švorčík, Carbon Nanostructures, Nanolayers, and Their Composites, *Nanomaterials*, 2021, **11**(9), 2368, DOI: 10.3390/nano11092368.
2 Q. He, Z. Wu, J. Li, R. Li, L. Zhang and Y. Liu, Quantitative and Biosafe Modification of Bifunctional Groups onto Carbon Dots by Click Chemistry, *J. Mater. Chem. B*, 2023, **11**(23), 5094–5100, DOI: 10.1039/D3TB00557G.
3 P. N. Navya, R. K. Jakku, H. Madhyastha, R. Ojha, S. Periasamy, M. Plebanski and S. K. Bhargava, Biogenic Carbon Dots Derived from the Microwave Carbonization of Amino Acid Mixture: Cellular Biocompatible, Biomolecular Probes, and Live Cell Imaging Agents, *J. Mater. Chem. B*, 2025, **13**(24), 7106–7117, DOI: 10.1039/D5TB00603A.
4 Y. Zhang, H. Qin, Y. Huang, F. Zhang, H. Liu, H. Liu, Z. J. Wang and R. Li, Highly Fluorescent Nitrogen and Boron Doped Carbon Quantum Dots for Selective and Sensitive Detection of Fe^{3+}, *J. Mater. Chem. B*, 2021, **9**(23), 4654–4662, DOI: 10.1039/d1tb00371b.
5 Z. Han, K. Wang, F. Du, Z. Yin, Z. Xie and S. Zhou, High Efficiency Red Emission Carbon Dots Based on Phenylene Diisocyanate for Trichromatic White and Red LEDs, *J. Mater. Chem. C*, 2018, **6**(36), 9631–9635, DOI: 10.1039/C8TC03497D.
6 R. Wang, K. Q. Lu, Z. R. Tang and Y. J. Xu, Recent Progress in Carbon Quantum Dots: Synthesis, Properties and Applications in Photocatalysis, *J. Mater. Chem. A*, 2017, 3717–3734, DOI: 10.1039/c6ta08660h.
7 D. Ozyurt, M. al Kobaisi, R. K. Hocking and B. Fox, Properties, Synthesis, and Applications of Carbon Dots: A Review, *Carbon Trends*, 2023, **12**, 100276, DOI: 10.1016/J.CARTRE.2023.100276.
8 S. Li, L. Li, H. Tu, H. Zhang, D. S. Silvester, C. E. Banks, G. Zou, H. Hou and X. Ji, The Development of Carbon Dots: From the Perspective of Materials Chemistry, *Materials Today*, 2021, **51**, 188–207, DOI: 10.1016/J.MATTOD.2021.07.028.
9 S. Tao, T. Feng, C. Zheng, S. Zhu and B. Yang, Carbonized Polymer Dots: A Brand New Perspective to Recognize Luminescent Carbon-Based Nanomaterials, *J. Phys. Chem. Lett.*, 2019, **10**(17), 5182–5188, DOI: 10.1021/ACS.JPCLETT.9B01384.
10 H. D. Almeida Gonzalez, G. R. Guerrero Porras, H. Vezin, L. Morales Alvarez, A. L. Corcho Valdés, L. J. Bravo Martínez, A. M. Díaz-García, D. González-Martínez, J. M. Moran-Mirabal, C. Murru, J. Deschamps, C. Iriarte-Mesa, Q. Jiang, F. Kleitz, L. F. Desdin-Garcia and M. Antuch, On the Enhanced Photocatalytic Activity of N-Doped Carbon Dots, *Catal. Sci. Technol.*, 2025, **15**(16), 4713–4726, DOI: 10.1039/D5CY00457H.
11 Z. L. Wu, Z. X. Liu and Y. H. Yuan, Carbon Dots: Materials, Synthesis, Properties and Approaches to Long-Wavelength and Multicolor Emission, *J. Mater. Chem. B*, 2017, 3794–3809, DOI: 10.1039/c7tb00363c.
12 E. Hastuti, C. Salsadilla, A. Y. Sari and U. Hikmah, The Hydrothermal Effect of Time and Temperature on the Synthesis of Carbon Dots (CDs) from Chicken Feathers, *IOP Conf. Ser. Earth Environ. Sci.*, 2024, **1312**(1), 012018, DOI: 10.1088/1755-1315/1312/1/012018.
13 G. Deme, A. Belay, D. M. Andoshe, G. Barsisa, D. Tsegaye, S. Tiruneh and C. Seboka, Effect of Hydrothermal Reaction Temperature on Fluorescent Properties of Carbon Quantum Dots Synthesized from Lemon Juice for Adsorption Applications, *J. Nanomater.*, 2023, **2023**(1), 1701496, DOI: 10.1155/2023/1701496.
14 T. Quaid, V. Ghalandari and T. Reza, Effect of Synthesis Process, Synthesis Temperature, and Reaction Time on Chemical, Morphological, and Quantum Properties of Carbon Dots Derived from Loblolly Pine, *Biomass*, 2022, **2**(4), 250–263, DOI: 10.3390/BIOMASS2040017/S1.
15 W. Fawaz, J. Hasian and I. Alghoraibi, Synthesis and Physicochemical Characterization of Carbon Quantum Dots Produced from Folic Acid, *Sci. Rep.*, 2023, **13**(1), 18641, DOI: 10.1038/s41598-023-46084-1.
16 R. B. González-González, L. T. González, M. Madou, C. Leyva-Porras, S. O. Martinez-Chapa and A. Mendoza, Synthesis, Purification, and Characterization of Carbon Dots from Non-Activated and Activated Pyrolytic Carbon

Black, *Nanomaterials*, 2022, **12**(3), 298, DOI: 10.3390/NANO12030298.

17 S. Jing, Y. Zhao, R. C. Sun, L. Zhong and X. Peng, Facile and High-Yield Synthesis of Carbon Quantum Dots from Biomass-Derived Carbons at Mild Condition, *ACS Sustainable Chem. Eng.*, 2019, **7**(8), 7833–7843, DOI: 10.1021/acssuschemeng.9b00027.

18 F. J. Cao, L. Wang, C. L. Feng, X. Lin and H. Feng, Synthesis of Polyurethane-Derived Nitrogen-Doped Carbon Dots for a High-Performance Fluorescence Bioimaging Probe, *RSC Adv.*, 2021, **11**(54), 34174–34180, DOI: 10.1039/d1ra06334k.

19 Z. Marković, S. Dorontić, S. Jovanović, J. Kovač, D. Milivojević, D. Marinković, M. Mojsin and B. Todorović Marković, Biocompatible Carbon Dots/Polyurethane Composites as Potential Agents for Combating Bacterial Biofilms: N-Doped Carbon Quantum Dots/Polyurethane and Gamma Ray-Modified Graphene Quantum Dots/Polyurethane Composites, *Pharmaceutics*, 2024, **16**(12), 1565, DOI: 10.3390/pharmaceutics16121565.

20 D. Seben, M. Toebe, A. D. Wastowski, K. Hofstätter, F. Volpatto, R. Zanella, O. D. Prestes and J. I. Golombieski, Water Quality Variables and Emerging Environmental Contaminant in Water for Human Consumption in Rio Grande Do Sul, Brazil, *Environ. Challenges*, 2021, **5**, 100266, DOI: 10.1016/J.ENVC.2021.100266.

21 Q. He, Z. Wu, J. Li, R. Li, L. Zhang and Y. Liu, Quantitative and Biosafe Modification of Bifunctional Groups onto Carbon Dots by Click Chemistry, *J. Mater. Chem. B*, 2023, **11**(23), 5094–5100, DOI: 10.1039/d3tb00557g.

22 Z. Marković, S. Dorontić, S. Jovanović, J. Kovač, D. Milivojević, D. Marinković, M. Mojsin and B. Todorović Marković, Biocompatible Carbon Dots/Polyurethane Composites as Potential Agents for Combating Bacterial Biofilms: N-Doped Carbon Quantum Dots/Polyurethane and Gamma Ray-Modified Graphene Quantum Dots/Polyurethane Composites, *Pharmaceutics*, 2024, **16**(12), 1565, DOI: 10.3390/pharmaceutics16121565.

23 L. Morbiato, M. Sbacchi, J. Dosso, P. Pengo, P. Gobbo, G. Filippini and M. Prato, Going Deep into the Surface Chemistry of Carbon Dots: Influence of Functional Groups on the Redox Abilities, *Small*, 2026, **22**(24), e14420, DOI: 10.1002/SMLL.202514420.

24 F. Bairamis and I. Konstantinou, Photocatalytic Degradation Pathways of the Valsartan Drug by TiO2 and G-C3N4 Catalysts, *Reactions*, 2022, **3**(1), 160–171, DOI: 10.3390/reactions3010012.

25 K. Akbar, E. Moretti and A. Vomiero, Carbon Dots for Photocatalytic Degradation of Aqueous Pollutants: Recent Advancements, *Adv. Opt. Mater.*, 2021, **9**(17), 2100532, DOI: 10.1002/adom.202100532.

26 M. A. Oturan and J. J. Aaron, Advanced Oxidation Processes in Water/Wastewater Treatment: Principles and Applications. A Review, *Crit. Rev. Environ. Sci. Technol.*, 2014, 2577–2641, DOI: 10.1080/10643389.2013.829765.

27 M. I. S. Dela Cruz, N. Thongsai, M. D. G. de Luna, I. In and P. Paoprasert, Preparation of Highly Photoluminescent Carbon Dots from Polyurethane: Optimization Using Response Surface Methodology and Selective Detection of Silver(I) Ion, *Colloids Surf., A*, 2019, **568**, 184–194, DOI: 10.1016/J.COLSURFA.2019.02.022.

28 Y. Jin, W. Tang, J. Wang, F. Ren, Z. Chen, Z. Sun and P. G. Ren, Construction of Biomass Derived Carbon Quantum Dots Modified TiO2 Photocatalysts with Superior Photocatalytic Activity for Methylene Blue Degradation, *J. Alloys Compd.*, 2023, **932**, 167627, DOI: 10.1016/J.JALLCOM.2022.167627.

29 F. z Zaman, A. Kumar, G. Yasin, F. O. Boakye, F. Muhammad, S. Iqbal, K. M. Alotaibi, L. Hou and C. Yuan, Enhanced Photocatalytic Degradation of Organic Dyes by Carbon Quantum Dots-ZnFe2O4 Composites, *J. Alloys Compd.*, 2024, **983**, 173860, DOI: 10.1016/J.JALLCOM.2024.173860.

30 A. B. Tegenaw, A. A. Yimer and T. T. Beyene, Boosting the Photocatalytic Activity of ZnO-NPs through the Incorporation of C-Dot and Preparation of Nanocomposite Materials, *Heliyon*, 2023, **9**(10), e20717, DOI: 10.1016/j.heliyon.2023.e20717.

31 B. A. Baitimbetova, K. S. Tolubayev, Yu. A. Ryabikin, D. O. Murzalinov, B. A. Zhautikov and G. S. Dairbekova, The Study of Carbon Nanomaterials by IR-Fourier Spectroscopy, Obtained by the Action of an Ultrasonic Field on Graphite, *Bull. Karaganda Univ. "Phys. Ser."*, 2022, **106**(2), 127–132, DOI: 10.31489/2022ph2/127-132.

32 N. Somaprakash, P. K. Badiya and V. Srinivasan, Green Synthesis of Fluorescent Carbon Dots as a Sustainable Catalyst for Thymol Blue Dye Degradation, *ChemPhysChem*, 2025, **26**(24), e202500526, DOI: 10.1002/cphc.202500526.

33 H. Ding, S. B. Yu, J. S. Wei and H. M. Xiong, Full-Color Light-Emitting Carbon Dots with a Surface-State-Controlled Luminescence Mechanism, *ACS Nano*, 2016, **10**(1), 484–491, DOI: 10.1021/acsnano.5b05406.

34 A. I. Ekimov and A. A. Onushchenko, Quantum Size Effect in Three-Dimensional Microscopic Semiconductor Crystals, *JETP Lett.*, 2023, **118**, S15–S17, DOI: 10.1134/S0021364023130040.

35 S. Dua, P. Kumar, B. Pani, A. Kaur, M. Khanna and G. Bhatt, Stability of Carbon Quantum Dots: A Critical Review, *RSC Adv.*, 2023, 13845–13861, DOI: 10.1039/d2ra07180k.

36 N. Luo, D. N. Wang and S. K. Ying, Hydrogen Bonding between Urethane and Urea: Band Assignment for the Carbonyl Region of FTi.r. Spectrum, *Polymer*, 1996, **37**(14), 3045–3047, DOI: 10.1016/0032-3861(96)89403-1.

37 Y. Ru, G. I. N. Waterhouse and S. Lu, Aggregation in Carbon Dots: Special Issue: Emerging Investigators, *Aggregate*, 2022, (6), e296, DOI: 10.1002/agt2.296.

38 C. Würth, M. Grabolle, J. Pauli, M. Spieles and U. Resch-Genger, Relative and Absolute Determination of Fluorescence Quantum Yields of Transparent Samples, *Nat. Protoc.*, 2013, **8**(8), 1535–1550, DOI: 10.1038/nprot.2013.087.

39 H. Jung, V. S. Sapner, A. Adhikari, B. R. Sathe and R. Patel, Recent Progress on Carbon Quantum Dots Based Photocatalysis, *Front. Chem.*, 2022, **5**(8), 3717, DOI: 10.3389/fchem.2022.881495.

40 B. Lapcikova and L. Lapcik *TG and DTG Study of Decomposition of Commercial PUR Cellular Materials*, 2011, vol. 28.
41 J. Ahn, C. Pealer and S. Kim, Analysis of Carbon Dots Synthesized at Different Hydrothermal Carbonization Temperatures and Their Ferric Ion Detection Performances, *Phys. Status Solidi B*, 2024, **261**(7), 2300345, DOI: 10.1002/pssb.202300345.
42 G. H. Al-Hazmi, M. S. Refat, M. G. El-Desouky and A. A. El-Bindary, Effective Adsorption and Removal of Industrial Dye from Aqueous Solution Using Mesoporous Zinc Oxide Nanoparticles via Metal Organic Frame Work: Equilibrium, Kinetics and Thermodynamic Studies, *Desalination Water Treat.*, 2022, **272**, 277–289, DOI: 10.5004/dwt.2022.28847.
43 M. Egorova, A. Tomskaya and S. A. Smagulova, Optical Properties of Carbon Dots Synthesized by the Hydrothermal Method, *Materials*, 2023, **16**(11), 4018, DOI: 10.3390/ma16114018.
44 N. Ghorai, S. Bhunia, S. Burai, H. N. Ghosh, P. Purkayastha and S. Mondal, Ultrafast Insights into Full-Colour Light-Emitting C-Dots, *Nanoscale*, 2022, **14**(42), 15812–15820, DOI: 10.1039/D2NR04642C.
45 H. D. Ibarra-Prieto, A. Garcia-Garcia, F. Aguilera-Granja, D. C. Navarro-Ibarra and I. Rivero-Espejel, One-Pot, Optimized Microwave-Assisted Synthesis of Difunctionalized and B–N Co-Doped Carbon Dots: Structural Characterization, *Nanomaterials*, 2023, **13**(20), 2753, DOI: 10.3390/NANO13202753.
46 D. G. Babar and S. S. Garje, Nitrogen and Phosphorus Co-Doped Carbon Dots for Selective Detection of Nitro Explosives, *ACS Omega*, 2020, **5**(6), 2710–2717, DOI: 10.1021/ACSOMEGA.9B03234.
47 Q. Zhang, R. Wang, B. Feng, X. Zhong and K. K. Ostrikov, Photoluminescence Mechanism of Carbon Dots: Triggering High-Color-Purity Red Fluorescence Emission through Edge Amino Protonation, *Nat. Commun.*, 2021, **12**(1), 6856, DOI: 10.1038/s41467-021-27071-4.
48 X. Li, S. Zhang, S. A. Kulinich, Y. Liu and H. Zeng, Engineering Surface States of Carbon Dots to Achieve Controllable Luminescence for Solid-Luminescent Composites and Sensitive Be2+ Detection, *Sci. Rep.*, 2014, **4**, 4976, DOI: 10.1038/srep04976.
49 M. Yu Khmeleva, K. A. Laptinskiy, P. S. Kasyanova, A. E. Tomskaya and T. A. Dolenko, Dependence of Photoluminescence of Carbon Dots with Different Surface Functionalization on Hydrogen Factor of Water, *Opt. Spectrosc.*, 2022, **130**(6), 697, DOI: 10.21883/eos.2022.06.54706.36-22.
50 A. P. Chowdhury, K. S. Anantharaju, K. Keshavamurthy and S. L. Rokhum, Recent Advances in Efficient Photocatalytic Degradation Approaches for Azo Dyes, *J. Chem.*, 2023, 9780955, DOI: 10.1155/2023/9780955.
51 A. Bożęcka, M. Orlof-Naturalna and M. Kopeć, Methods of Dyes Removal from Aqueous Environment, *J. Ecol. Eng.*, 2021, **22**(9), 111–118, DOI: 10.12911/22998993/141368.
52 I. Khan, K. Saeed, I. Zekker, B. Zhang, A. H. Hendi, A. Ahmad, S. Ahmad, N. Zada, H. Ahmad, L. A. Shah, T. Shah and I. Khan, Review on Methylene Blue: Its Properties, Uses, Toxicity and Photodegradation, *Water*, 2022, **14**(2), 242, DOI: 10.3390/w14020242.
53 R. Saleh and A. Taufik, Photo-Fenton Degradation of Methylene Blue in the Presence of Au-Fe 3 O 4/Graphene Composites under UV and Visible Light at near Neutral PH: Effect of Coexisting Inorganic Anion, *Environ. Nanotechnol. Monit. Manage.*, 2019, **11**, 100221, DOI: 10.1016/j.enmm.2019.100221.
54 M. Antonopoulou, M. Papadaki, I. Rapti and I. Konstantinou, Photocatalytic Degradation of Pharmaceutical Amisulpride Using G-C3N4 Catalyst and UV-A Irradiation, *Catalysts*, 2023, **13**(2), 226, DOI: 10.3390/catal13020226.
55 C. Xia, S. Zhu, T. Feng, M. Yang and B. Yang, Evolution and Synthesis of Carbon Dots: From Carbon Dots to Carbonized Polymer Dots, *Adv. Sci.*, 2019, **6**(23), 1901316, DOI: 10.1002/advs.201901316.
56 W. N. A. Guerra, J. M. T. Santos and L. R. R. De Araujo, Decolorization and Mineralization of Reactive Dyes by a Photocatalytic Process Using ZnO and UV Radiation, *Water Sci. Technol.*, 2012, **66**(1), 158–164, DOI: 10.2166/wst.2012.154.
57 A. Okunola, J. T. Kim and R. Raja Gupta, Identification and Kinetic Tracking of Degradation Intermediates of Methylene Blue Using HPLC-MS to Map the Al/Ce-ZnO Photocatalytic Reaction Pathway, , 2025.
58 H. R. Rajabi, O. Khani and M. Shamsipur, Vatanpour, V. High-Performance Pure and Fe3 + -Ion Doped ZnS Quantum Dots as Green Nanophotocatalysts for the Removal of Malachite Green under UV-Light Irradiation, *J. Hazard. Mater.*, 2013, **250–251**, 370–378, DOI: 10.1016/j.jhazmat.2013.02.007.
59 N. M. Mahmoodi, M. Oveisi, A. M. Arabi and B. Karimi, Cadmium Selenide Quantum Dots: Synthesis, Characterization, and Dye Removal Ability with UV Irradiation, *Desalination Water Treat.*, 2016, **57**(35), 16552–16558, DOI: 10.1080/19443994.2015.1079259.
60 Y. Wang, Y. Liu, H. Zhang, X. Duan, J. Ma, H. Sun, W. Tian and S. Wang, Carbonaceous Materials in Structural Dimensions for Advanced Oxidation Processes, *Chemical Soc. Rev.*, 2025, **54**, 2436, DOI: 10.1039/d4cs00338a.
61 H. Gnaser, M. R. Savina, W. F. Calaway, C. E. Tripa, I. V. Veryovkin and M. J. Pellin, Photocatalytic Degradation of Methylene Blue on Nanocrystalline TiO 2: Surface Mass Spectrometry of Reaction Intermediates, *Int. J. Mass Spectrom.*, 2005, **245**(1–3), 61–67, DOI: 10.1016/j.ijms.2005.07.003.
62 T. Shirafuji, Y. Ishida, A. Nomura, Y. Hayashi and M. Goto, Reaction Mechanisms of Methylene-Blue Degradation in Three-Dimensionally Integrated Micro-Solution Plasma, *Jpn. J. Appl. Phys.*, 2017, **56**, 06HF02, DOI: 10.7567/JJAP.56.06HF02.
63 N. Ishak, P. Galář, R. Mekkat, M. Grandcolas and M. Šoóš, Fine-Tuning Photoluminescence and Photocatalysis: Exploring the Effects of Carbon Quantum Dots Synthesis and Purification on g-C3N4, *Colloids Surf., A*, 2025, **706**, 1–14, DOI: 10.1016/j.colsurfa.2024.135789.